JHEP PROCEEDINGS

International Europhysics Conference on HEP

Higgs production plus two jets at hadron colliders

V. Del Duca*

I.N.F.N., Sez. di Torino, via P. Giuria, 1 - 10125 Torino, Italy
E-mail: delduca@to.infn.it

W. Kilgore

Physics Department, Brookhaven National Laboratory
Upton, New York 11973, U.S.A.
E-mail: kilgore@bnl.gov

C. Oleari and D. Zeppenfeld

Department of Physics, University of Wisconsin
Madison, WI 53706, U.S.A.
E-mail: oleari@pheno.physics.wisc.edu, dieter@pheno.physics.wisc.edu

C.R. Schmidt

Department of Physics and Astronomy, Michigan State University
East Lansing, MI 48824, USA
E-mail: schmidt@pa.msu.edu

Abstract: In this talk we present a calculation of Higgs production via gluon fusion in association with two jets, including the full top-quark mass dependence, and compare it to the large top-mass limit. We find that the large top-mass limit is a good approximation as long as the Higgs mass is smaller than the top quark pair mass, and the jet transverse energies are smaller than the top mass. In addition, we compare Higgs production via gluon fusion and via weak-boson fusion, and consider final-state distributions, like the rapidity interval between the jets and the jet-jet azimuthal decorrelation, which may allow us to distinguish one fusion process from the other.

1. Higgs production at hadron colliders

At the Large Hadron Collider (LHC) a Higgs boson is expected to be produced mainly by gluon fusion or weak-boson fusion (WBF) [1, 2]. The WBF channel, even though numerically smaller, is interesting because it is expected to provide information on Higgs boson couplings [3]. In addition, it is theoretically simple to analyse, since it produces the

*Speaker.

Higgs boson via t-channel W or Z exchange, in association with two forward quark jets, $qQ \to qQH$. QCD radiative corrections to WBF are known to be small [4] [1], and thus this process promises small systematic errors.

The gluon-fusion channel is much more challenging. The Higgs boson couples to gluons via a quark loop, thus every calculation to a given loop accuracy in QCD implies one more heavy-quark loop. Since the scattering amplitude is proportional to the quark mass squared [2], in the numerical evaluation of the production rate it suffices to consider only the top quark. Inclusive Higgs production via gluon fusion, $g\,g \to H$, is known at NLO in QCD, including the full m_t dependence [5], and the NLO corrections are known to be large ($\mathcal{O}(100\%)$). At next-to-next-to-leading order (NNLO), inclusive Higgs production via gluon fusion is known only in the $m_t \to \infty$ limit [6], for which the top-quark loop reduces to an effective $H\,g\,g$ coupling, and the calculation reduces from three to two loops. However, in the intermediate Higgs mass range, which is favoured by electroweak precision data [7], the Higgs boson mass m_H is small compared to the top-quark pair threshold and the large m_t limit promises to be an adequate approximation.

$H + 1$ jet production via gluon fusion is known at leading order (LO), including the full m_t dependence [8], and at NLO in the $m_t \to \infty$ limit [9]. Also in this case the NLO corrections are known to be large, roughly of the same order as in the inclusive case. $H + 2$ jet production via gluon fusion was previously known at LO, but only in the $m_t \to \infty$ limit [10]. Both in $H + 1$ jet and in $H + 2$ jet production, phase space regions open up where one or several of the kinematical invariants are of the order of, or exceed, the top-quark mass, i.e. regions of large Higgs boson or jet transverse momenta, or regions where dijet invariant masses become large. These regions may invalidate the $m_t \to \infty$ limit, even in the intermediate Higgs mass range, but yield a rather small contribution to inclusive Higgs production. However, in $H + 1$ jet or in $H + 2$ jet production one may require a Higgs-jet mass or a dijet mass to be large (e.g. in $H + 2$ jet production we may require the dijet mass to be large, in order to compare with the large dijet mass of the two forward jets in the WBF process), then it is important to evaluate the extent to which the $m_t \to \infty$ limit holds. Therefore, in this talk we review the results of a recent calculation of $H + 2$ jet production, including the full m_t dependence [11], where the issues above are analysed.

2. Higgs production plus two jets at the LHC

Gluon fusion and weak-boson fusion ($qQ \to qQH$ production via t-channel exchange of a W or Z), are expected to be the dominant sources of $H + 2$ jet events at the LHC. The impact of the former on LHC Higgs phenomenology is determined by the relative size of these two contributions. We evaluate the $H + 2$ jet cross section through a minimal set of cuts on the final-state partons, which anticipates LHC detector capabilities and jet finding

[1] The t-channel singlet exchange ensures that at next-to-leading order (NLO) no gluon is exchanged in the t-channel, unless the incoming quarks are of equal flavour.

[2] The Yukava coupling is proportional to m_q, and there is an additional factor of m_q due to the compensation of the chirality flip, induced by the insertion of a single scalar $Hq\bar{q}$ vertex.

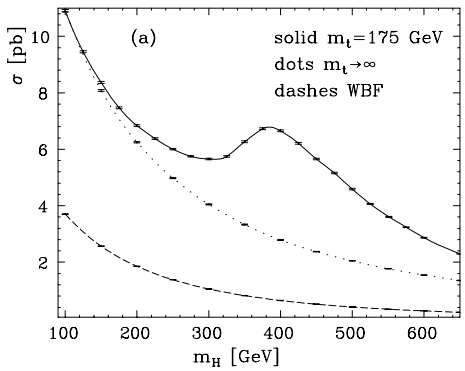

Figure 1: $H + 2$ jet cross sections in pp collisions at $\sqrt{s} = 14$ TeV as a function of the Higgs boson mass. Results are shown for gluon-fusion processes induced by a top-quark loop with $m_t = 175$ GeV and in the $m_t \to \infty$ limit, and for weak-boson fusion. The cuts of Eq. (2.1) have been used.

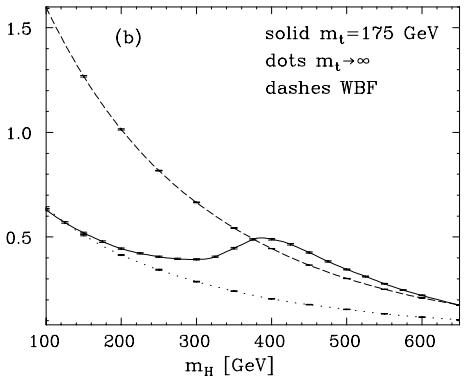

Figure 2: Same as Fig. 1, but with the WBF selection of cuts of Eqs. (2.1) and (2.2)

algorithms,

$$p_{j\perp} > 20 \text{ GeV}, \quad |\eta_j| < 5, \quad R_{jj} > 0.6\,, \tag{2.1}$$

where $p_{j\perp}$ is the transverse momentum of a final state parton and R_{jj} describes the separation of the two partons in the pseudo-rapidity η versus azimuthal angle plane $R_{jj} = \sqrt{\Delta\eta_{jj}^2 + \phi_{jj}^2}$. Expected $H + 2$ jet cross sections at the LHC are shown in Fig. 1, as a function of the Higgs boson mass, m_H. The three curves compare results for the expected Standard Model gluon-fusion cross section at $m_t = 175$ GeV (solid line) with the large-m_t limit (dotted line), computed using the heavy-top effective Lagrangian, and with the WBF cross section (dashed line). Error bars indicate the statistical errors of the Monte Carlo integration. Cross sections correspond to the sum over all Higgs decay modes: finite Higgs width effects are included. The factorization scale was set to $\mu_f = \sqrt{p_{1\perp}\, p_{2\perp}}$, and α_S was taken to be $\alpha_S(M_Z) = 0.12$. Different choices of renormalization and factorization scales have been discussed in Ref. [11], where a strong sensitivity of the $H + 2$ jet cross section on the renormalization scale was found.

Fig. 1 shows cross sections within the minimal cuts of Eq. (2.1). The gluon-fusion contribution dominates because the cuts retain events with jets in the central region, with relatively small dijet invariant mass. In order to assess background levels for WBF events, it is more appropriate to consider typical tagging jet selections employed for WBF studies [12]. This is done in Fig. 2 where, in addition to the cuts of Eq. (2.1), we require

$$|\eta_{j1} - \eta_{j2}| > 4.2\,, \qquad \eta_{j1} \cdot \eta_{j2} < 0\,, \qquad m_{jj} > 600 \text{ GeV}\,, \tag{2.2}$$

i.e. the two tagging jets must be well separated, they must possess a large dijet invariant mass, and must reside in opposite detector hemispheres. With these selection cuts the weak-boson fusion processes dominate over gluon fusion by about 3/1 for Higgs boson masses in the 100 to 200 GeV range. This means that a relatively clean separation of

weak-boson fusion and gluon-fusion processes will be possible at the LHC, in particular when extra central-jet-veto techniques are employed to further suppress semi-soft gluon radiation in QCD backgrounds [12].

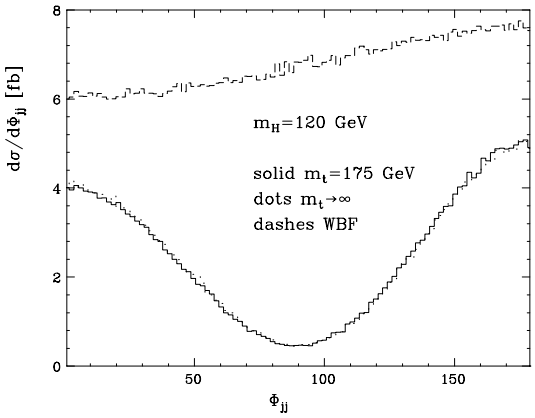

Figure 3: Azimuthal-angle distribution between the two final jets, with the WBF cuts of Eqs. (2.1) and (2.2). Results are shown for gluon-fusion processes induced by a top-quark loop with $m_t = 175$ GeV and in the $m_t \to \infty$ limit, computed using the heavy-top effective Lagrangian, and for weak-boson fusion.

A conspicuous feature of the $H + 2$ jet gluon-fusion cross sections in Figs. 1 and 2 is the threshold enhancement at $m_H \approx 2\,m_t$, an effect which is familiar from the inclusive gluon-fusion cross section. Well below the threshold-peak region, the large m_t limit provides an excellent approximation to the total $H + 2$ jet rate from gluon fusion, at least when considering the total Higgs production rate only. Fig. 2 also implies that the approximation provided by the large m_t limit at Higgs boson masses below about 200 GeV is excellent. Thus the large dijet invariant mass, $m_{jj} > 600$ GeV, and the concomitant large parton center-of-mass energy do not spoil the $m_t \to \infty$ approximation. A hint to understand that can be found in the high-energy limit, which is appropriate for the large dijet mass case. In the high-energy limit only Feynman diagrams with gluon exchange in the t channel are relevant. When taking in addition the large m_t limit, the same diagrams contribute. Thus, if the high-energy limit is appropriate to describe the region of large dijet mass, so is the combined high-energy and large m_t limit. The only difference is in the high-energy coefficient functions, or impact factors, which in the combined limit lose the information on the m_t dependence. Finally, as shown in Ref. [11], the large m_t limit works well in the intermediate Higgs mass range, as long as jet transverse momenta stay small: $p_{j\perp} \lesssim m_t$.

Turning now to the issue of differentiating between gluon fusion and WBF processes, a characteristic of WBF events is the large rapidity separation of the two tagging jets, a feature which is not shared by $H + 2$ jet events arising from gluon fusion. The plots of the rapidity separation of the jets [11] show indeed that for the inclusive cuts of Eq. (2.1) jets coming from WBF events are produced preferentially with a rather large rapidity separation, while jets coming from gluon fusion events are produced mostly in the central rapidity region. Accordingly, when WBF cuts (2.1) and (2.2) are implemented the jets coming from gluon fusion events are depleted, thus the jet separation cut is one of the most effective means of enhancing WBF processes with respect to gluon fusion.

Another jet-angular correlation, which allows to distinguish gluon fusion from weak-boson fusion, is the azimuthal angle between the two jets, ϕ_{jj}. The distributions for gluon-fusion and WBF processes are shown in Fig. 3. In the WBF process $qQ \to qQH$, the matrix element squared $|\mathcal{A}_{\rm WBF}|^2$ is proportional to $\hat{s}m_{jj}^2$, with $\hat{s}$ the squared parton center-of-mass energy and m_{jj} the dijet invariant mass. Since the dependence of m_{jj}^2 on

ϕ_{jj} is mild, we have the flat behavior depicted in Fig. 3. The azimuthal-angle distribution of the gluon-fusion process is instead characteristic of the CP-even operator $HG_{\mu\nu}G^{\mu\nu}$, where $G_{\mu\nu}$ is the gluon field strength tensor. This effective coupling can be taken as a good approximation for the ggH coupling in the large-m_t limit. Infact the large-m_t limit (dotted line) is almost indistinguishable from the $m_t = 175$ GeV result (solid line). Not only does the ϕ_{jj} correlation allow us to distinguish WBF from gluon fusion, it can also be used as a tool to investigate the tensor structure of the WWH coupling. Infact, if we suppose that there is an anomalous (i.e. non Standard Model) WWH coupling, which in the low-energy effective theory can be modeled through higher-dimensional operators, the ϕ_{jj} correlation discriminates between a CP-even coupling, which behaves like the ggH coupling, and a CP-odd coupling, which would hinder configurations where the jets are aligned or back-to-back [13].

References

[1] G. L. Bayatian *et al.*, CMS Technical Proposal, report CERN/LHCC/94-38x (1994); R. Kinnunen and D. Denegri, CMS NOTE 1997/057; R. Kinnunen and A. Nikitenko, CMS TN/97-106; R. Kinnunen and D. Denegri, [hep-ph/9907291].

[2] ATLAS Collaboration, ATLAS TDR, report CERN/LHCC/99-15 (1999).

[3] D. Zeppenfeld, R. Kinnunen, A. Nikitenko and E. Richter-Was, *Phys. Rev.* **D 62** (2000) 013009 [hep-ph/0002036].

[4] T. Han and S. Willenbrock, *Phys. Lett.* **B 273** (1991) 167.

[5] A. Djouadi, N. Spira and P. Zerwas, *Phys. Lett.* **B 264** (1991) 440; M. Spira, A. Djouadi, D. Graudenz and P.M. Zerwas, *Nucl. Phys.* **B 453** (1995) 17 [hep-ph/9504378]; S. Dawson, *Nucl. Phys.* **B 359** (1991) 283.

[6] S. Catani, D. de Florian and M. Grazzini, *J. High Energy Phys.* **05** (2001) 025 [hep-ph/0102227]; R. Harlander and W. Kilgore, *Phys. Rev.* **D 64** (2001) 013015 [hep-ph/0102241].

[7] See e.g. LEP Electroweak Working Group, LEPEWWG Note 2001-01 (2001) and http://lepewwg.web.cern.ch/LEPEWWG/.

[8] R. K. Ellis, I. Hinchliffe, M. Soldate and J. J. van der Bij, *Nucl. Phys.* **B 297** (1988) 221.

[9] D. de Florian, M. Grazzini and Z. Kunszt, *Phys. Rev. Lett.* **82** (1999) 5209 [hep-ph/9902483].

[10] S. Dawson and R. P. Kauffman, *Phys. Rev. Lett.* **68** (1992) 2273; R. P. Kauffman, S. V. Desai and D. Risal, *Phys. Rev.* **D 55** (1997) 4005 [hep-ph/9610541].

[11] V. Del Duca, W. Kilgore, C. Oleari, C. Schmidt and D. Zeppenfeld, [hep-ph/0105129]; [hep-ph/0108030].

[12] D. Rainwater, R. Szalapski and D. Zeppenfeld, *Phys. Rev.* **D 54** (1996) 6680; D. Rainwater and D. Zeppenfeld, *Phys. Rev.* **D 60** (1999) 113004, Erratum-ibid. *Phys. Rev.* **D 61** (2000) 099901; D. Rainwater, PhD thesis, [hep-ph/9908378]; T. Plehn, D. Rainwater and D. Zeppenfeld, *Phys. Rev.* **D 61** (2000) 093005.

[13] T. Plehn, D. Rainwater and D. Zeppenfeld, [hep-ph/0105325].